Materials Science Forum *Online: 2008-09-09*
ISSN: 1662-9752, Vols. 595-598, pp 753-762
doi:10.4028/www.scientific.net/MSF.595-598.753

On the effect of surface treatment to improve oxidation resistance and conductivity of metallic interconnects for SOFC in operating conditions

S. Fontana[1], M. Vuksa[1,2], S. Chevalier[1], G. Caboche[1], P. Piccardo[2]

[1] Institut Carnot de Bourgogne, UMR 5209 CNRS - Université de Bourgogne, 9 avenue Alain Savary, BP 47870, F-21078 Dijon Cedex (France)

[2] DCCI, Universita di Genova, via Dodecaneso 31, I 16146 Genova (Italy)

Keywords: SOFC, reactive element, interconnect, MOCVD

Abstract. Due to the reduction of operating temperature from 1000°C to 800°C, chromia forming alloys are the best candidates for interconnects in Solid Oxide Fuel Cells (SOFCs). These interconnects have to be operational in service conditions, at 800°C in air (cathode side) and in humidified hydrogen (anode side). The performance of the interconnect stainless steels is limited by the oxide scale formation (chromia), the low electronic conductivity of this scale and the possible volatility of chromium oxides. In the field of high temperature oxidation of metals, it is well known that the addition of a nanometric layer made of reactive element oxide such as, La_2O_3, Nd_2O_3 and Y_2O_3 by MOCVD (Metal Organic Chemical Vapor Deposition) on alloy surface resulted in an important improvement in the high temperature oxidation resistance. These coatings are made on metallic alloys in order to form perovskite oxides such as $LaCrO_3$, $NdCrO_3$ and $YCrO_3$, which are expected to present a good conductivity at 800°C in air. However, this temperature looks somewhat too low to guarantee the formation of perovskite oxides and thus to improve the oxidation resistance and electrical conductivity. In fact, XRD analyses revealed that for Y_2O_3 coatings, perovskite oxides were not formed after oxidation in air at 800°C for 100 hours. The goal of this study is to perform pre-oxidation at 1000°C for 2 hours in air under atmospheric pressure on coated Crofer22APU to pre-form perovskite phases. The so-prepared perovskite were tested in a thermobalance in air. Experiments performed in H_2/10%H_2O under 150 mbar at 800°C validated the coating influence from the anode side as well as the cathode side. The corrosion products were analyzed after 100 hours ageing at 800°C by SEM, EDX, and XRD. ASR (Area Specific Resistance) was measured for the same times and temperature in air.

Introduction

Solid Oxide Fuel Cells (SOFCs) are considered as a clean, low-pollutant technology to generate electricity from a variety of fuel such as hydrogen or methane. A single-cell SOFC is composed of a porous cathode and a porous anode separated by a gas imperviousness ion-conducting electrolyte. The main function of the interconnects is to provide the electrical connection between single cells. They also act as physical barrier between the reducing and the oxidizing atmospheres. The most important characteristics required for the interconnect is high electronical conductivity with an area-specific resistance (ASR) below 0.1 $\Omega.cm^2$, an excellent oxidation, sulfidation and carbon cementation resistance in both atmospheres for 40 000 h at operating temperature (around 800°C) and a thermal expansion coefficient (TEC) matching those of the electrodes and the electrolyte, around $10.5x10^{-6}$ K^{-1} [1-4]. Many researches have enabled to decrease the operating temperature of the SOFC to 800°C, allowing then the use of metallic interconnects instead of ceramics. Metallic

materials have higher electrical and thermal conductivities, are easier to fabricate, and, in general, cheaper than ceramic interconnects [4, 5, 6].

Among the tested metallic materials, ferritic chromia-forming alloys are the best candidates. Despite a TEC close to that of the ceramic components of the cell and the formation at 800°C of a protective chromia Cr_2O_3 scale, it can transform in volatile chromium species, such as CrO_3 or $CrO_2(OH)_2$ leading to the lost of its protectiveness and then the degradation of the fuel cell [7-9]. Although alumina or silica scales can provide superior oxidation resistance, they have much lower electrical conductivities, making them inappropriate for interconnects.

The improvement of electrical conductivity and oxidation resistance of chromia-forming alloys by the addition of a nanometric reactive element oxide (REO) layer has been well documented [10-13]. At 800°C, the best effect on alloys is the elements of the beginning of the lanthanide group and the yttrium. These elements are known to reduce the oxidation rate, to improve the oxide-scale adherence and to prevent Cr oxide vaporization. Their main role consists of changing the diffusion mechanism during the chromia scale formation, from outward diffusion of chromium ions to inward diffusion of oxygen ions.

In this study and in a previous work [13], La_2O_3, Y_2O_3 and Nd_2O_3 coatings were deposited on Crofer22APU [14] by Metal-Organic Chemical Vapor Deposition (MOCVD) in order to form perovskite oxides such as $LaCrO_3$, $YCrO_3$ and $NdCrO_3$ which present a good conductivity at 800°C. In the case of Y_2O_3-coating, this temperature is to low to form perovskite oxides and thus to improve the oxidation resistance and the electrical conductivity. That is the reason why a part of this work consists of studying the effect of pre-oxidation [15] at 1000°C for 2 h in air on the oxidation behavior in air at 800°C of uncoated and coated Crofer22APU.

Isothermal oxidation experiments were performed at 800°C for 100 h in air under atmospheric pressure (for the cathode side) and H_2/10%H_2O under 150 mbar (for the anode side). The coatings, the pre-oxidized samples and the corrosion products were carefully analyzed by scanning electron microscopy (SEM), energy dispersive X-ray (EDX) analyses and X-ray diffraction (XRD). The electrical resistivity measurements of the oxidized alloy were performed on uncoated and coated samples in air in order to determine the ASR parameter.

Experimental Procedures

The metallic material used in this study was a ferritic stainless steels, Crofer22APU. This alloy was provided by ThyssenKrupp VDM. The nominal composition is given in Table 1. This alloy is composed of a homogeneous microstructure with a grain size in the range 60–80 μm.

Table.1 Crofer22APU composition in weight (%)

Wt. %	C	Cr	Fe	Mn	P	S	Ti	La
Crofer 22 APU	0.005	22	Bal	0.5	0.016	0.002	0.08	0.06

The samples were cut in squares of 1 x 1 cm and about 2.5 mm of thickness; prior to deposition, the samples were polished from 240-grit silicon carbide up to 1 μm with diamond paste. They were finally cleaned in ethanol in an ultrasonic bath and dried.

The reactive elements (La, Nd and Y) were introduced onto the polished sample surface as thin oxide films prepared by Metal Organic Chemical Vapor Deposition (MOCVD) technique. β-diketonate powders (tris-2,2,6,6-tetramethyl-3,5-heptanedionato (tmhd) of La, Nd or Y) were used

as metal-organic precursors. The detail process of deposition was described elsewhere [13, 16]. This technique enables to deposit thin nanostructured oxide films of about 100-200 nm thick.

In a previous work [13], uncoated and coated samples were oxidized at 800°C for 100 h in air under atmospheric pressure (laboratory air). In order to evaluate the coating influence on corrosion resistance in H_2/H_2O, specimens were oxidized in controlled $H_2/10\%H_2O$ gas mixture under 150 mbar at 800°C for 100 h. Coated and uncoated specimen were pre-oxidized for 2 h at 1000°C in air under atmospheric pressure. The so-prepared samples were then studied at 800°C in air under atmospheric pressure for 100 h. During these experiments, the samples were continuously weighted in a thermobalance in order to get the oxidation kinetics.

The surface oxide morphologies after oxidation were analyzed using a "JEOL JSM-6400F" scanning electron microscope (SEM) equipped with a field emission gun (FEG). This equipment, coupled with an energy dispersive X-ray spectrometer was used to determine the morphology and the chemical analyses of the corrosion products. The oxides formed after ageing were characterized by X-ray diffraction (XRD) using Cu K_α (λ=1.154 nm) radiation with an incidence angle of 1°. The area-specific resistance (ASR) parameter reflects the electrical properties of the oxide layers. The electrical resistivity measurements of the oxidized alloy were only performed in air on uncoated and coated samples without pre-oxidation. The detailed process of the measurement and the calculation are described elsewhere [13].

Results and discussion

Oxidation test in air and in $H_2/10\%H_2O$. In a previous work [13], the oxidation test of uncoated and coated Crofer22APU in air at 800°C showed that the oxidation kinetics obeyed a parabolic rate law and that the reactive element oxide improved significantly the corrosion resistance of the alloy. Kinetics of scale formation on uncoated and coated Crofer22APU for 100 h in $H_2/10\%H_2O$ under 150 mbar are presented in Fig. 1. All specimens obey a parabolic rate law. The presence of a reactive element oxide on the surface reduces the parabolic rate constants, k_p, determined from the slope of the plot of $\Delta m/A$ versus $t^{1/2}$ [17]. Table 2 gives the values of the parabolic rate constant and of the mass gain in $H_2/10\%H_2O$. A comparison is made with the values determined in air from reference [13].

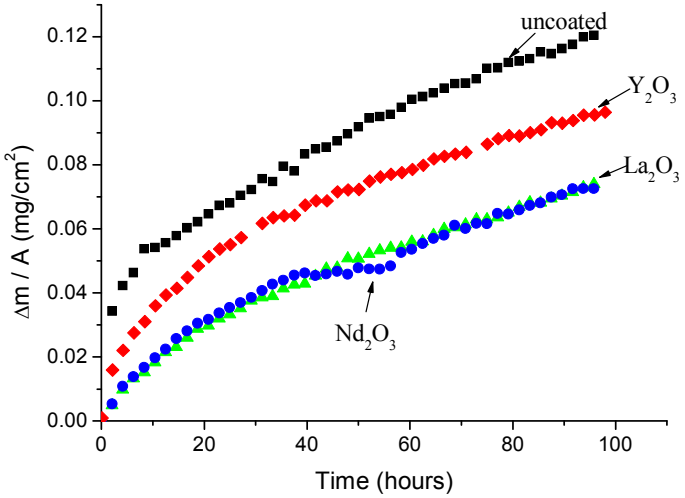

Fig. 1. Kinetics (for 100h) of coated and uncoated Crofer22APU at 800°C in $H_2/10\%H_2O$

Whatever the coatings, the oxidation resistance is improved. In air, the coating effect does not depend on the nature of the reactive element. The mass gain is reduced of 20 % for coated specimens. The mass gain of uncoated Crofer22APU oxidized in $H_2/10\%H_2O$ is increased of 25% compare to the same specimen oxidized in air. It illustrates that the mechanism of formation of oxide scale in air and in $H_2/10\%H_2O$ is different. Moreover, in $H_2/10\%H_2O$ the effect of the coating depends on the selected reactive element. Indeed, in comparison with uncoated alloys, La_2O_3 and the Nd_2O_3 coatings gave the same beneficial effect; the mass gain is reduced of approximately 38%, whereas the mass gain is only decreased by 20% in the case of Y_2O_3 coating.

The effects of reactive element oxide coatings were clearly evidenced on scale morphologies after oxidation in air [13]. In the case of uncoated Crofer22APU oxidized in air, a spinel phase (Cr, Mn)3O4 very closed to Cr1.5Mn1.5O4 (ICDD card n°33-0892) covering an sub-scale of chromia (ICDD card n°38-1479) was detected. For La2O3, Nd2O3-coatings, the oxide scale after 100 h in air at 800°C was composed of a triple layered microstructure with spinel oxide on the top of surface, covering a widely developed under-scale of perovskite phase (LaCrO3 (ICDD card n°33-0701) or NdCrO3 (ICDD card n°39-1429)). The third layer was composed of chromia. Finally, for the Y2O3-coated specimen, the surface presented an homogeneously distributed presence of cracks. XRD analyses revealed the presence of yttria (ICDD card n°41-1105) and spinel, but no perovskite phase YCrO3. Thus, at 800°C for 100h in air, Y2O3 coatings did not react with chromia in order to form perovskite phase [13]. The presence of yttria (or LaCrO3 or NdCrO3) improved the corrosion resistance by changing the diffusion mechanism during the chromia scale formation from outward diffusion of the chromium ions to inward diffusion of the oxygen ions [**7**].

Table.2 kp values and total mass-gain after 100 hours at 800°C

	Coating	kp ($g^2.cm^{-4}.s^{-1}$)	$\Delta m/A$ ($mg.cm^{-2}$)
Air (atmospheric pressure)	**Without coatings**	2.6×10^{-14}	0.098
	La_2O_3 coating	8.9×10^{-15}	0.077
	Nd_2O_3 coating	1.0×10^{-14}	0.076
	Y_2O_3 coating	1.1×10^{-14}	0.074
$H_2/10\%H_2O$ (150 mbar)	**Without coatings**	2.9×10^{-14}	0.122
	La_2O_3 coating	1.9×10^{-14}	0.075
	Nd_2O_3 coating	1.7×10^{-14}	0.071
	Y_2O_3 coating	2.5×10^{-14}	0.097
Air after pre-oxidation	**Without coatings**	1.4×10^{-15}	0.023
	La_2O_3 coating	1.9×10^{-15}	0.027
	Nd_2O_3 coating	1.3×10^{-15}	0.022
	Y_2O_3 coating	1.5×10^{-15}	0.025

Fig. 2 reveals the surface morphologies of uncoated and coated samples aged for 100h in $H_2/10\%H_2O$ at 800°C. The morphology of the oxide scale is very different than that of the same sample aged in air [13]. In the air, the oxide scale on uncoated and coated samples is homogeneous. The microstructure of the outer grains is typical spinel phases, covering an underscale composed of smaller grains. In $H_2/10\%H_2O$, in all case, the grain boundaries of the alloy remained visible on the oxidized surface. The oxide scale on the uncoated sample is heterogeneous. The grain boundaries are decorated by some clusters of platelets (filament shape). Between grain boundaries, the oxide scale is composed of two parts. Many nodules decorated by whiskers are present and a second zone

is composed of smaller grains. The whiskers and the platelets are enriched in Cr and Mn; some traces of Ti are detected. For uncoated and coated samples, XRD analyses (Table 3) show the presence of a spinel $(Cr,Mn)_3O_4$ and chromia; in addition, they reveal the presence of MnO_2 (ICDD card n° 07-0230). For the La_2O_3-coated sample, the oxide scale is homogenous and is composed of small equiaxed grains. At the alloy grains boundaries, the oxide scale is slightly thicker and some nodules are present. XRD analyses revealed the presence of a perovskite phase, $LaCrO_3$. In the case of Nd_2O_3-coating, the surface and the crystalline phases are similar to those obtained for the La_2O_3-coating. However, nodules are present between the grain boundaries of the alloy. XRD analyses identify some traces of Nd_2O_3, indicating that, in H_2/H_2O atmosphere, this oxide does not react completely with chromia in order to form a perovskite phase. Like in air, the morphology of the Y_2O_3-coated specimen is slightly different but does not present any cracks. Typical spinel phases decorated the alloy grain boundaries and are present at the top of the oxide scale. The deepest layer is made up of finer grains. XRD indicate the presence of yttria without perovskite phase. As in air, at 800°C in H_2/H_2O, yttria does not react with Cr_2O_3 to form $YCrO_3$.

Table.3 Phases identified by XRD analyses on the surface of uncoated and coated samples of Crofer22APU after 100h at 800°C in air under atmospheric pressure and in $H_2/10\%H_2O$ under 150 mbar

Atmosphere	Coating	XRD phases
Air (atmospheric pressure)	Without coating	Cr_2O_3, $(Cr,Mn)_3O_4$
	La_2O_3 coating	Cr_2O_3, $LaCrO_3$, $(Cr,Mn)_3O_4$
	Nd_2O_3 coating	$NdCrO_3$, $(Cr,Mn)_3O_4$
	Y_2O_3 coating	Y_2O_3, $(Cr,Mn)_3O_4$
$H_2/10\%H_2O$ (150mbar)	Without coating	$(Cr,Mn)_3O_4$, MnO_2, Cr_2O_3
	La_2O_3 coating	$(Cr,Mn)_3O_4$, MnO_2, Cr_2O_3, $LaCrO_3$
	Nd_2O_3 coating	$(Cr,Mn)_3O_4$, MnO_2, Cr_2O_3, $NdCrO_3$, Nd_2O_3
	Y_2O_3 coating	$(Cr,Mn)_3O_4$, MnO_2, Cr_2O_3, Y_2O_3

Electrical conductivity measurement. The measurements of the ASR parameter were made only in air (cathode side). The study of electric properties of oxide scale on uncoated and coated Crofer22APU showed that the presence of reactive element oxide modified the ASR values compared to the uncoated alloy. The electrical parameter depends on the selected coating. In the case of the uncoated alloy, after 100 h at 800°C, the ASR parameter is equal to 0.086 $\Omega.cm^2$, thus this alloy designed specifically for interconnect was well adapted because its ASR parameter is below 0.1 $\Omega.cm^2$. In the case of La_2O_3 coating, it is clear that the presence of a perovskite like $LaCrO_3$ which has a low resistivity (2.9 Ω.cm at 1000°C) [2], improves the electric conductivity of the oxide scale; in fact, after 100 h at 800°C, the ASR parameter is only 0.004 $\Omega.cm^2$. However, in the case of Y_2O_3-coating, yttria is still present after 100h at 800°C in air. Its important resistivity (10^{11} Ω.cm at 800°C [2]), higher than the resistivity of chromia (10^2 Ω.cm at 800°C [2]) and the spinel $Cr_{1.5}Mn_{1.5}O_4$ (20 Ω.cm at 800°C [2]), explains the increase of ASR parameter (ASR=0.252 $\Omega.cm^2$). In the case of Nd_2O_3 coating, there is an improvement of the electric conductivity, but the value of the ASR parameter (0.016 $\Omega.cm^2$) is higher than that La_2O_3 coating.

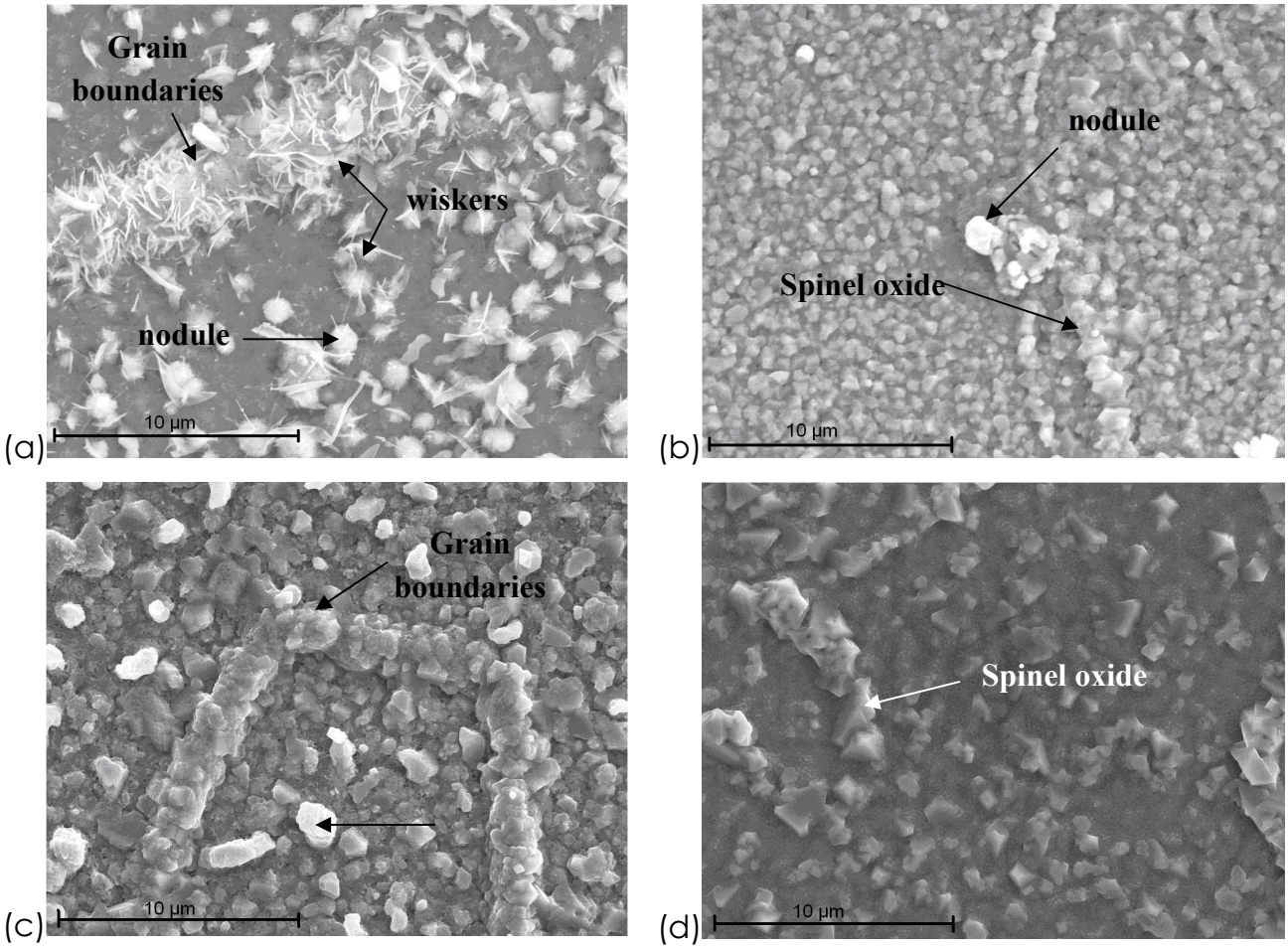

Fig. 2. SEM observations of Crofer22APU oxidised in H_2/10%H_2O at 800°C for 100 h: (a) uncoated, (b) La_2O_3-coated, (c) Nd_2O_3-coated and (d) Y_2O_3-coated

Effect of a pre-oxidation on the oxidation resistance. In order to form perovskite phases like $LaCrO_3$, $YCrO_3$ or $NdCrO_3$, coated samples were pre-oxidized for 2 h at 1 000°C in air under atmospheric pressure. Pre-oxidation was also performed on the uncoated Crofer22APU. The mass gain for pre-oxidized, uncoated and coated samples after 2h at 1000°C is equal to 0.24 mg.cm^2. Fig. 3 shows the surface morphologies of uncoated and coated samples after 2 h at 1000°C in air. The microstructure of the oxide scale is very different compared to that observed after 100h at 800°C. The oxide is very thin, homogeneous and composed of very fine oxide grains (around 600 nm) enriched in Cr en Mn. Furthermore, some nodules are scattered over the surface, and Ti traces are detected around theses nodules. It is interesting to notice that the oxide around the nodules look like spinel phases. XRD analyses on the surface of uncoated and coated samples of Crofer22APU after 2h at 1000°C are reported in table 4. For uncoated alloy, chromia and a spinel $(Cr,Mn)_3O_4$ are detected. The morphologies of the coated Crofer22APU after pre-oxidation are very similar to those of the uncoated alloy. For the La_2O_3-coated and Nd_2O_3 sample, the oxide layer is composed of spinel $(Cr,Mn)_3O_4$, chromia and a perovskite phase ($LaCrO_3$ or $NdCrO_3$). As after ageing in air at 800°C for 100 h, after 2 hours in air at 1000°C, yttria is still present on the Y_2O_3-coated alloy. It does not totally react with chromia in order to form perovskite. This was already observed by Chevalier et al. [18].

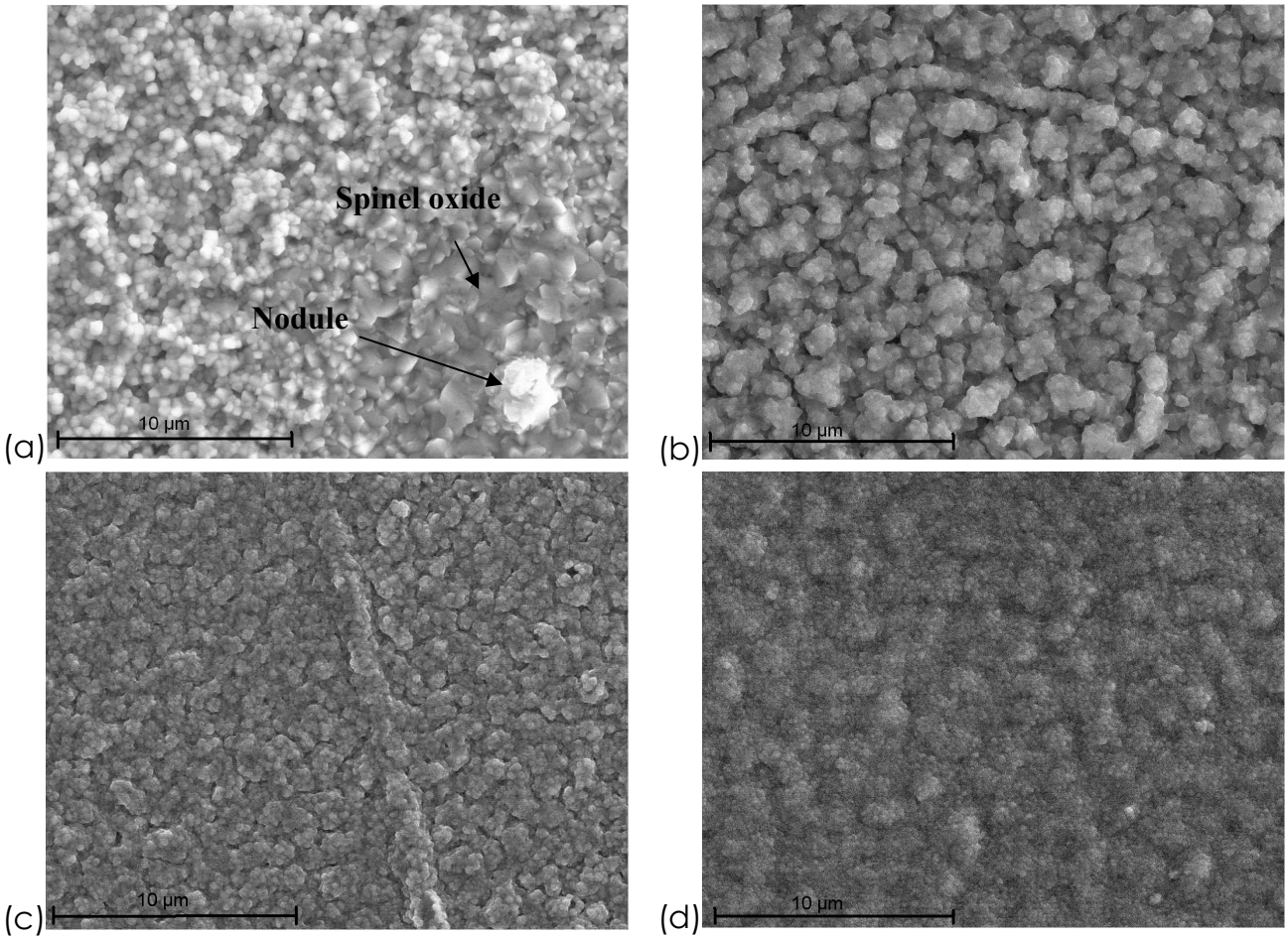

Fig. 3. SEM observations of Crofer22APU pre-oxidised in air at 1000°C for 2h: (a) uncoated, (b) La_2O_3-coated, (c) Nd_2O_3-coated and (d) Y_2O_3-coated

Table.4 Phases identified by XRD analyses on the surface of pre-oxidized (2h at 1000°C) samples of uncoated and coated Crofer22APU before and after oxidation at 800°C for 100h

Coating	Treatment	XRD phases
Without coatings	pre-oxidation	Cr_2O_3, $(Cr,Mn)_3O_4$
	pre-oxidation and oxidation	Cr_2O_3, $(Cr,Mn)_3O_4$
La_2O_3 coating	pre-oxidation	Cr_2O_3, $(Cr,Mn)_3O_4$, $LaCrO_3$
	pre-oxidation and oxidation	Cr_2O_3, $(Cr,Mn)_3O_4$, $LaCrO_3$
Y_2O_3 coating	pre-oxidation	Y_2O_3, Cr_2O_3, $(Cr,Mn)_3O_4$
	pre-oxidation and oxidation	$YCrO_3$, Cr_2O_3, $(Cr,Mn)_3O_4$
Nd_2O_3 coating	pre-oxidation	Cr_2O_3, $(Cr,Mn)_3O_4$, $NdCrO_3$
	pre-oxidation and oxidation	Cr_2O_3, $(Cr,Mn)_3O_4$, $NdCrO_3$

The kinetics of scale formation on pre-oxidized samples during oxidation at 800°C for 100 h in air under atmospheric pressure are presented in Fig. 4. As previously, the curves show parabolic kinetics. Since the mass gain after 100 h at 800°C is very low, deviation form parabolic law was sometimes observed. Based upon these oxidation experiments, it is clear that the pre-oxidation at 1000°C for 2 hours leads to a beneficial effect. If compared to the untreated samples, the mass gain during oxidation at 800°C for 100 h is reduced of approximately 70% for the pre-oxidized

specimens. Nevertheless, after 100 hours, the beneficial effect of reactive element is not evident, at least on the oxidation rate.

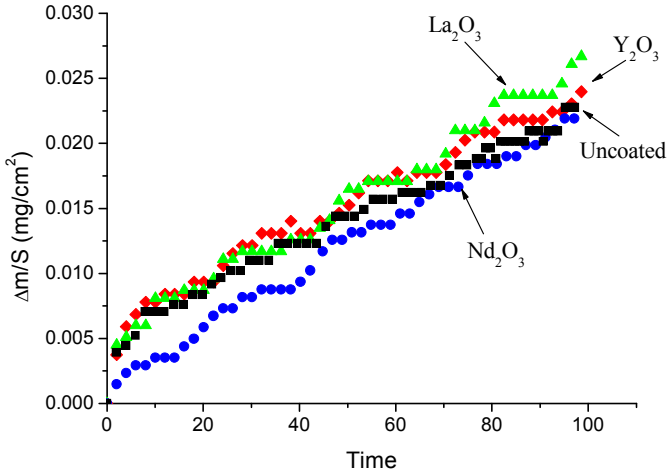

Fig. 4. Kinetics (for 100h) of pre-oxidised sample of coated and uncoated Crofer22APU at 800°C in air under atmospheric pressure

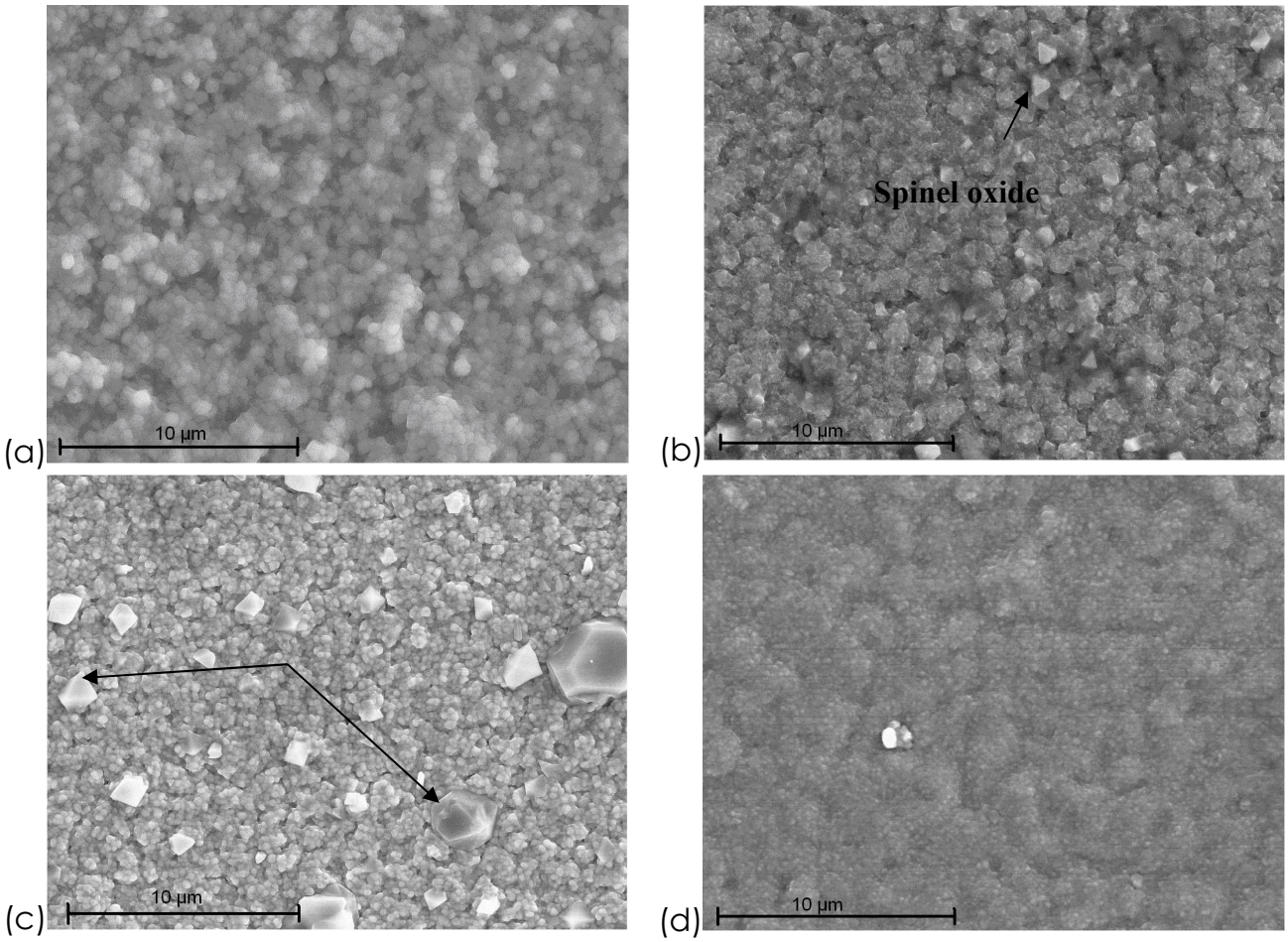

Fig. 5. SEM observations of pre-oxidised sample of Crofer22APU oxidised in air at 800°C for 100h: (a) uncoated, (b) La_2O_3-coated, (c) Nd_2O_3-coated and (d) Y_2O_3-coated

Fig. 5 shows the surface morphologies of pre-oxidized samples and then aged after 100 h at 800°C in air under atmospheric pressure. For the uncoated alloy, the surface is not very different compared to that after pre-oxidation; the oxide scale is very thin and very homogeneous; the only distinction is

that the nodules disappeared. XRD analyses (Table 4) show that the oxide scale is mainly composed of a spinel, (Cr, Mn)$_3$O$_4$, with some traces of chromia. In the case of pre-oxidized La_2O_3-coated alloy, there are some spinel oxides covering an under-scale made of smaller grains of $LaCrO_3$. A spinel (Cr, Mn)$_3$O$_4$, a perovskite of $LaCrO_3$ and traces of chromia are detected by XRD. For the Nd_2O_3 coating, the morphology and the crystalline phases are similar to those obtained for heat-treated La_2O_3-coated Crofer22APU. The spinel crystallites are bigger. Finally, the morphology of heat-treated Y_2O_3-coated alloy is similar than that of the uncoated alloy, but the oxide grains are thinner. The major difference is given by XRD analyses which reveal only the presence of a perovskite phase $YCrO_3$ and no more yttria. So, after 2 h at 1000°C and 100 h at 800°C in air, yttria reacted with chromia in order to form the perovskite phase, $YCrO_3$. Further experiments will be necessary to evaluate the perovskite phase influence on the ASR parameter.

Conclusion

High temperature oxidation tests, performed on uncoated and coated Crofer22APU, showed that the reactive element had a beneficial effect on the oxidation behaviour in air and in H_2/10%H_2O. The coatings composed of a thin reactive element oxide such as, La_2O_3, Nd_2O_3 and Y_2O_3 resulted in an important decrease of the oxide growth rate. Contrary to oxidation in air, in the H_2/10%H_2O atmosphere, the effect of the coating depends on the selected reactive element. Furthermore, for the uncoated alloy, the oxidation is more important in H_2/10%H_2O than in air. This illustrates that the steam plays an important role in the oxidation mechanism. The first objective of these coatings was to form perovskite oxide with the chromia growing layer because perovskite exhibit better conductivities than chromia. The La_2O_3-coated Crofer22APU which form a perovskite phase after 100h at 800°C, has the best ASR parameter (0.004 $\Omega.cm^2$). Nevertheless, for the Y_2O_3-coating, the ASR parameter is not acceptable; this is correlated to the fact that no perovskite phases were detected by XRD analyses after 100h at 800°C. In order to form perovskite oxide, preliminary pre-oxidation at 1000°C for 2 hours were envisaged. They improve the oxidation resistance. The still open question is to know if it is better to pre-cover the surface of the alloy with a perovskite layer or to let its formation during the ageing of the material at 800°C. Moreover, ASR measurements in H_2/10%H_2O validate the coating influence. In the future, it will be interesting to evaluate the oxidation resistance of pre-oxidized alloy (2 h at 1000°C in air) under H_2/10%H_2O.

References

[1] W.Z. Zhu, S.C. Deevi: Material Research Bulletin 38 (2003), 957-972.

[2] W.Z. Zhu, S.C. Deevi: Material Sciences and Engineering A348 (2003), 227-243.

[3] V. Shemet, J. Piron-Abellan, W. J. Quadakkers, L. Singheiser, in: N. Sammes, A. Smirnova, O. Vasylyev (Eds.), Fuel cell technologies: State and Perspectives, Springer, Netherlands, 2005, pp. 97-106.

[4] L. Antoni, Materials Sciences Forum 461-464 (2004), 1073-1090.

[5] J. W. Fergus, Materials Science and Engineering A397 (2005), 271-283.

[6] K. Przybylski, T. Brylewski, J. Morgiel, Materials Sciences Forum 461-464 (2004), 1099-1106

[7] W.J. Quadakkers, J. Piron-Abellan, V. Shemet, L. Singheiser, Materials at high temperatures 20 (2) 115-127.

[8] K. Huang, P. Y. Hou, J. B. Goodenough, Solid State Ionics 129 (2000), 237-250.

[9] P. Berthod, Oxidation of Metals 64 (2005) 235-252.

[10] D.E. Alman, P. D. Jablonski, International Journal of Hydrogen Energy 32 (2007) 3743-3753.

[11] P. Y. Hou, J. Stringer, Materials Science and Engineering A202 (1995), 1-10.

[12] T. Brylewski, K. Przybylski, J. Morgiel, Materials Chemistry and Physics 81 (2003), 434-437.

[13] S. Fontana, R. Amendola, S. Chevalier, P. Piccardo, G. Caboche, M. Viviani, R. Molins, M. Sennour, Journal of power sources (2007), 171 (2007) 652-662

[14] P. Huczkowski, N. Christiansen, V. Shemet, J. Piron-Abellan, L. Singheiser, W. J. Quadakkers, Materials and Corrosion 55 (2004) 825-830.

[15] S. Chevalier, S. Ched'Homme, A. Bekaddour, K. Amilain-Basset, L. Buisson, Materials and Corrosion 58 (2007), 353-361.

[16] S. Chevalier, G. Bonnet, J.P. Larpin, Applied Surface Science 167 (2000), 125-133.

[17] B. Pierragi, Oxidation of Metals 27 (1987) 177-185.

[18] S. Chevalier, J.P. Larpin, Acta Materiala 50 (2002) 3105-3114.